

Altered Expression of *GJD2* Messenger RNA and the Coded Protein Connexin 36 in Negative Lens–induced Myopia of Guinea Pigs

Qirong Zhu, BSc, OD,¹ Guoyuan Yang, MD, PhD,² Bingjie Chen, MD, PhD,² Fengyang Liu, MSc, OD,³ Xia Li, BSc, OD,¹ and Longqian Liu, MD, PhD^{2*}

SIGNIFICANCE: Decreased expression of the retinal *GJD2* gene messenger RNA (mRNA) and connexin 36 (Cx36) protein in the guinea pig negative lens–induced myopia (LIM) model suggests their involvement in local retinal circuits regulating eye growth.

PURPOSE: Previous studies suggest that the *GJD2* gene and Cx36 protein encoded by the *GJD2* gene play important roles in retinal signaling pathways and eye development. The aim of this study was to investigate the changes in *GJD2* mRNA and Cx36 protein expression in the guinea pig lens–induced myopia model.

METHODS: Four-week-old guinea pigs were randomly divided into two groups. Animals in the experimental group were fitted with monocular –10 D lenses; and animals in the control group, with monocular plano lenses. Biometric measurements, including the spherical equivalent refractive error and axial length, were monitored. Animals were killed after 0, 1, 2, and 3 weeks of treatment, and their retinas were isolated. Retinal *GJD2* mRNA and Cx36 protein expression levels were assessed by quantitative real-time polymerase chain reaction and Western blot analysis, respectively.

RESULTS: Spherical equivalent refractive error values indicated that negative lens–treated eyes became significantly more myopic than plano lens–treated eyes ($P = .001$), consistent with their longer axial lengths compared with those of control eyes. Both *GJD2* mRNA and Cx36 protein expression levels were decreased in the retinas of negative lens–treated eyes compared with levels in the retinas of plano lens–treated eyes, although there were differences in the timing; *GJD2* mRNA, levels were significantly decreased after 1 and 2 weeks of treatment ($P = .01$ and $P = .004$, respectively), whereas Cx36 protein expression was significantly decreased after only 1 week ($P = .01$).

CONCLUSIONS: That both retinal *GJD2* mRNA and Cx36 protein expression levels were decreased after induction of myopia with negative lenses points to retinal circuits involving Cx36 in myopia development in the guinea pig.

Optom Vis Sci 2020;97:1080–1088. doi:10.1097/OPX.0000000000001611

Copyright © 2020 The Author(s). Published by Wolters Kluwer Health, Inc. on behalf of the American Academy of Optometry.

This is an open-access article distributed under the terms of the Creative Commons Attribution-Non Commercial-No Derivatives License 4.0 (CCBY-NC-ND), where it is permissible to download and share the work provided it is properly cited. The work cannot be changed in any way or used commercially without permission from the journal.

Supplemental Digital Content: Direct URL links are provided within the text.

OPEN SDC



Author Affiliations:

¹Department of Optometry and Visual Science, West China Hospital, Sichuan University, Chengdu, Sichuan, China

²Department of Ophthalmology, West China Hospital, Sichuan University, Chengdu, Sichuan, China

³Department of Optometry, Guizhou Provincial People's Hospital, Guiyang, Guizhou, China

*b.q15651@hotmail.com

Myopia describes the refractive error in which parallel light from distant objects focuses in front of the retina, in the absence of accommodation.¹ This condition is a product of the axial length of an eye being too long for its refractive power. In 2016, it was estimated that the global prevalence of myopia would rise dramatically to reach 49.8%, which equates to approximately 5 billion people. Of these individuals, 9.8%, or nearly 1 billion people, are expected to develop high myopia.² The annual cost of managing myopia for Singapore adults has been estimated to be \$775 million.³ In the United States, the estimated annual direct cost for refractive correction has been estimated to be at least \$3.8 billion.⁴ Apart from this substantive socioeconomic burden,⁵ complications such as glaucoma, retinal detachment, and maculopathy⁶ associated with high myopia may considerably compromise visual acuity and thus the quality of life of those affected.⁷

Studies involving myopia animal models, including guinea pigs, tree shrews, chickens, mice, and rhesus monkeys, have generated important information on early eye growth patterns and refractive development^{8–12} and have also contributed to our understanding of the underlying biochemical signaling pathways linking the retina

to the sclera.^{13,14} These studies and other research have led to the general consensus that most myopia is a product of environmental influences combined with genetic factors.¹⁵ Several studies, including population and independent genome-wide association studies with large sample sizes, have identified significant associations between single-nucleotide polymorphisms on chromosome 15q14, which is proximal to the *GJD2* gene, and refractive errors.^{16–20} However, a functional role of *GJD2* in myopia has not yet been established.

The connexin 36 (Cx36) protein, which is encoded by the *GJD2* gene, is a component of gap junctions that allows for direct communication via small molecules, cytosolic ions, and electrical impulses between neighboring cells.²¹ Cx36 has been described in many animals, including humans, guinea pigs, mice, and rabbits, being the main connexin protein and widely distributed across various organs and tissues.^{22,23} In the retina of the eye, immunological studies have confirmed that Cx36 is expressed in both the inner and outer plexiform layers, is present on cone pedicles and OFF cone bipolar cells,²⁴ and provides links between amacrine cells²⁵ and between dendrites of α -type ganglion cells.²⁶ Deletion of Cx36

leads to decreases in coupling between neuronal cells in the retina and alterations in retinal functions, including reductions in b-waves and disruption of signal transmission in the visual pathway.^{27,28}

It is plausible that such disruption of visual signaling could affect eye development and so induce refractive errors.^{29,30} Other studies have shown that dopamine, an important retinal neurotransmitter that has been linked to refractive development and myopia, plays an important role in Cx36 phosphorylation and dephosphorylation reactions. In addition, research has revealed that prolonged dark adaptation can change the distribution, expression, and phosphorylation of Cx36, which interacts with dopamine as a regulator in this process.³¹

A limited number of studies have reported that uncoupling of gap junctions containing Cx35 (the chicken homolog of Cx36) prevents myopia in chicks, possibly by modifying some actions of dopamine and/or nitric oxide.³² Given this observation and previous genetic research, as cited previously, linking the *GJD2* gene with myopia, and the molecular biological data pointing to critical roles of Cx36 in both photoreceptors and neuronal signaling pathways of the retina, the present study aimed to further investigate their roles in myopia using the guinea pig as a mammalian model. Guinea pigs have been extensively used in myopia research because they have relatively large eyes and are easy to handle for ocular biometrical measurements. Changes in both retinal *GJD2* transcript and Cx36 protein levels during myopia development were evaluated.

METHODS

Animal Model

Four-week-old pigmented guinea pigs were provided by the Laboratory Animal Center of Sichuan University in Chengdu, Sichuan Province, China. The guinea pigs weighed between 180 and 220 g. The animals were raised in an air-conditioned room with an ambient temperature of 20 to 25°C, a relative humidity of 45 to 65%, and a 12-hour on, 12-hour off, light-dark cycle. Cage illumination was provided by fluorescent lamps, with three peak emissions at 440, 550, and 620 nm, with the average illuminance within the animal cages being approximately 300 to 400 lux. The animals were provided free access to water and food supplemented with vitamin C.

The experimental procedures and animal treatments were conducted in accordance with the Regulations of Animal Experiment Guidelines and adhered to the Association for Research in Vision and Ophthalmology guidelines for the use of animals in ophthalmic and vision research. The study protocol was approved by the Animal Care and Use Committee of Sichuan University.

Animals were divided randomly into two groups, an experimental group and a control group. In total, there were 24 animals in each group. Each guinea pig in the experimental group wore a -10 D lens in front of their right eye for 1, 2, or 3 weeks to induce myopia while allowing for normal eyelid function (Appendix Fig. A1, available at <http://links.lww.com/OPX/A461>). The choice of lens power (-10 D) was to ensure that hyperopic defocus was maintained throughout the longest, 3-week treatment period. The -10.00 D lenses were made from PMMA (King Tak & Jia Run Co., Beijing, China), with the following parameters: an overall diameter of 17.00 mm, an optical zone diameter of 11.5 mm, a posterior (inside) optical radius of 7.50 mm, and an outside optical radius of 8.927 mm. Each guinea pig in the control group wore a plano lens in front of their right eye instead of the negative lens.

Routine lens checks were performed three times each day. When scratches on the optic zone of a lens were detected, it was immediately replaced.^{33,34} The lenses were removed temporarily (for <3 minutes) for daily cleaning under dim illumination to minimize exposure of the animals to visual stimuli during this time. The other non-lens-wearing eye of each guinea pig in both groups functioned as a contralateral control eye.

Ocular and Biometric Measurements

During this process, the animals were carefully held without anesthesia. In both groups, biometric measurements, including spherical equivalent refractive error, corneal radius of curvature, and axial length measurements, were taken immediately before the initiation of the lens treatment, as well as after 1, 2, and 3 weeks of treatment. Two research optometrists blinded to the treatments of the animals completed all of the measurements independently.

Refractive errors were measured by retinoscopy. Before measurement, each eye of each animal received up to four drops of 0.5% tropicamide/0.5% phenylephrine ophthalmic solution^{35–37} (Santen Pharmaceutical Co., Ltd., Osaka, Japan), spaced 5 minutes apart, to achieve mydriasis and cycloplegia. The optometrists used a streak retinoscope (66 Vision-Tech Co., Ltd., Suzhou, China) at a 67-cm working distance in a dark environment to perform the test. The refractive errors of each animal were measured in triplicate. Results are presented as the spherical equivalent (in diopters), which represents the mean values of the horizontal and vertical meridians, after correction for the working distance; that is, 1.50 D was subtracted from the average of the raw data.

The corneal radius of curvature was measured using a portable automatic keratometer (Suor SW-100, Tianjin, China). Both the horizontal and vertical corneal radii of curvature were measured when four clear and steady red dots were simultaneously visible. The mean of eight measurements was taken as the final result.

An ophthalmic ultrasonography instrument (11 MHz probe; Aviso, Cournon-d'Auvergne, France), set to A-scan mode, was used to measure the following ocular axial parameters³⁸: anterior chamber depth, lens thickness, and vitreous chamber depth, after first instilling topical 0.4% oxybuprocaine hydrochloride eye drops (Santen Pharmaceutical Co., Ltd.) to anesthetize the cornea. Axial lengths were derived as the sum of these components. The ultrasound velocities for the different ocular media were as follows: 1557.5 m/s for the aqueous humor, 1723.3 m/s for the lens, and 1540 m/s for the vitreous body.³⁸ When performing these measurements, the examiner placed the tip of the probe directly on the surface of the cornea, orientating the probe to ensure that the ultrasound beam passed approximately perpendicularly through each of the ocular surfaces.

Tissue Extraction

At each of the experimental time points, that is, 0, 1, 2, and 3 weeks, a subset of six guinea pigs from each of the two treatment groups was killed, and retinal tissue was collected. In all cases, the guinea pigs were killed immediately after the completion of biometric measurements via an intraperitoneal injection of 10% chloral hydrate (200 mg/kg; Boster Biological Technology Co., Ltd., Wuhan, China). The treated eye of each animal was then rapidly enucleated and placed on an inverted ice-cold culture dish for dissection. Briefly, a 3- to 5-mm incision was made on the lateral canthus, isolating the connective tissue. The optic nerve was then cut, and the eyeball was isolated. The cornea was removed from the eye by making a circumferential cut at the limbus under a dissecting microscope. After gently removing the lens and vitreous body, to

reveal the three layers making up the wall of the posterior eyecup, the retina was then carefully separated from the underlying choroid. The retinal pigment epithelium was left behind with the choroid. The retinal samples were immediately frozen in liquid nitrogen until subsequently analyzed. In total, six retinal samples (one per animal) were collected at each time point from each group for quantitative real-time polymerase chain reaction (n = 3) and Western blot (n = 3) analyses.

Quantitative Real-time Polymerase Chain Reaction

Total RNA was isolated from retinal samples using TRIzol reagent (Invitrogen, Carlsbad, CA) according to the manufacturer's instructions. After quantifying the RNA concentrations with a NanoDrop spectrophotometer (NanoDrop Technologies, Wilmington, DE), reverse transcription was performed to synthesize complementary DNA from 1 µg of total RNA using a GoldScript complementary DNA kit (Invitrogen) following the manufacturer's instructions. The sequences of the quantitative real-time polymerase chain reaction primers for *GJD2* and β-actin are listed in Table 1. β-Actin served as an internal control. The specificity of the primers was confirmed by melting curve analysis. Quantitative real-time polymerase chain reaction was conducted on a qTOWER 2.2 machine (Ana lytik Jena, Jena, Germany). Polymerase chain reaction amplification was conducted using 20 µL of SsoFast EvaGreen Supermix (Bio-Rad Laboratories Inc., Hercules, CA). Three independent polymerase chain reaction runs were undertaken on each sample. All of the PCR assays were conducted with an initial denaturation phase at 95°C for 35 seconds followed by 35 cycles of denaturation at 95°C for 5 seconds, annealing at 60°C for 35 seconds, and extension at 72°C for 40 seconds. Relative *GJD2* expression was calculated by using the 2^{-ΔΔCt} method: ΔΔCt = (Ct, *GJD2*-Ct, β-actin)_{experimental group} - (Ct, *GJD2*-Ct, β-actin)_{control group}.

Western Blotting

Total protein samples were extracted from the retinas using RIPA lysis and extraction buffer containing 1% Halt proteinase inhibitor cocktail (Thermo Scientific, Waltham, MA) for 30 minutes on ice; the reaction products were then centrifuged for 15 minutes at 13,000g at 4°C. The protein concentration was measured using a bicinchoninic acid protein assay kit (Beyotime Institute of Biotechnology, Shanghai, China) based on the manufacturer's instructions. All the samples were mixed with 5× loading buffer (Beyotime Institute of Biotechnology) and boiled at 100°C for 5 minutes. Subsequently, the protein samples were electrophoresed on 12% sodium dodecyl sulfate–polyacrylamide gels (Bio-Rad Laboratories Inc.) using 30 µg of protein from each retinal sample; the stacking gel was run for 30 minutes at 80 V, and the separating gel was run for 60 minutes at 120 V. The bands were then transferred to polyvinylidene difluoride membranes (Millipore,

Billerica, MA) at 250 mA for 90 minutes at 4°C. Next, the membranes were blocked with 5% nonfat dry milk in 0.1% Tween-20 (TBST; 2 mmol/L Tris-HCl, 50 mmol/L NaCl, pH 7.5) for 2 hours at room temperature and then incubated overnight at 4°C with two primary antibodies simultaneously: a rabbit anti-Cx36 polyclonal antibody (1:1000; LC-C101642; Lifespan, Seattle, WA) and a mouse monoclonal anti-β-actin antibody (1:2000; ab6276; Abcam, Cambridge, United Kingdom), which served as the internal reference. The membranes were then washed three times with TBST (15 minutes each time) before being incubated simultaneously with the corresponding secondary antibodies, horseradish peroxidase–conjugated goat antirabbit (1:2000; BA1054) and goat antimouse (1:2000; BA1050) IgG (both from Boster Biological Technology), for 1 hour at room temperature. The membranes were then again washed three times (15 minutes each time) with TBST. An enhanced chemiluminescence detection system (EMD Millipore, Billerica, MA) was used to capture the protein bands, which were exposed onto negative film, developed, and fixed. The film was scanned and subsequently analyzed using Quantity One Imaging Software (version 1; Bio-Rad Laboratories, Inc.).

Statistical Analysis

Statistical analysis was performed using GraphPad Prism 5.0 (GraphPad Prism Software, Inc., San Diego, CA). The data for the treated and contralateral eyes, as well as for the interocular differences (treated eye vs. contralateral eye), are reported as the mean ± SEM. Statistical significance was defined as P < .05. After testing for normality, the data for the lens-treated eyes (including the ocular biometric parameters, *GJD2* messenger RNA levels, and Cx36 protein expression levels) of the experimental and control groups were compared using independent *t* tests. All *P* values were from two-sided tests. Comparisons of the results collected at different time points for each group were performed by one-way ANOVA followed by Bonferroni correction.

RESULTS

Ocular Parameters of the Guinea Pigs

Before myopia induction (0 weeks), no significant differences in spherical equivalent refractive error, axial length, or corneal radius of curvature were observed between the groups, nor did these measurements differ between the eyes of any individual guinea pig (P > .05, paired *t* test). The results for both the right eyes and left eyes in each group are summarized in Table 2. The changes in spherical equivalent refractive error, axial length, and corneal radius of curvature over time are also shown as interocular differences in Fig. 1. The -10 D lenses were successful in inducing myopia, such that by the end of the 3-week treatment period the experimental group showed significantly greater myopic shift,

TABLE 1. Primers sequence of real-time polymerase chain reaction

Gene	Product size (bp)	Forward primer (5'–3')	Reverse primer (5'–3')
<i>GJD2</i>	186	CAGAGCCAGATTGTTTAGAAG	GGGACTGAAGCCATAGAG
β-Actin	87	TTCTAGCGGACTGTACTAC	CAATCTCATCTCGTTTCTG

bp = base pairs.

TABLE 2. Results of ocular biometric parameters, including SER, AL, ACD, LT, and VCD (mean ± SEM), in guinea pigs monocularly fitted with negative lenses (in the experimental group) or plano lenses (in the control group) for 0 to 3 weeks

Group	Treatment	Time point	No. eyes	SER (D)	CRC (mm)	AL (mm)	ACD (mm)	LT (mm)	VCD (mm)
EXP	−10 D lens	0 wk	24	3.64 ± 0.83	3.48 ± 0.11	7.83 ± 0.13	1.18 ± 0.03	3.21 ± 0.03	3.49 ± 0.09
		1 wk	18	1.47 ± 0.67*	3.52 ± 0.16	8.10 ± 0.21†	1.19 ± 0.04	3.22 ± 0.05	3.81 ± 0.10†
		2 wk	12	−0.58 ± 0.46*	3.49 ± 0.14	8.32 ± 0.11†	1.21 ± 0.03	3.25 ± 0.04	3.87 ± 0.10†
		3 wk	6	−1.54 ± 0.60*	3.45 ± 0.16	8.47 ± 0.16†	1.22 ± 0.05	3.27 ± 0.05	3.93 ± 0.12†
		Changes (3 − 0 wk)	NA	−5.18 ± 0.24	−0.03 ± 0.08	0.64 ± 0.05	0.04 ± 0.03	0.06 ± 0.04	0.44 ± 0.03
CON	Plano lens	0 wk	24	3.59 ± 1.06	3.49 ± 0.10	7.86 ± 0.14	1.16 ± 0.04	3.19 ± 0.03	3.51 ± 0.11
		1 wk	18	3.54 ± 0.88	3.54 ± 0.13	7.89 ± 0.15	1.17 ± 0.02	3.21 ± 0.03	3.52 ± 0.13
		2 wk	12	3.34 ± 0.82	3.52 ± 0.11	7.92 ± 0.12	1.17 ± 0.04	3.22 ± 0.06	3.53 ± 0.12
		3 wk	6	3.20 ± 0.97	3.45 ± 0.12	8.01 ± 0.24	1.19 ± 0.05	3.27 ± 0.06	3.53 ± 0.15
		Changes (3 − 0 wk)	NA	−0.39 ± 0.21	−0.04 ± 0.08	0.15 ± 0.04	0.03 ± 0.02	0.08 ± 0.04	0.02 ± 0.03
EXP	No lens	0 wk	24	3.68 ± 0.97	3.49 ± 0.10	7.85 ± 0.12	1.19 ± 0.04	3.21 ± 0.03	3.46 ± 0.06
		1 wk	18	3.50 ± 0.94	3.53 ± 0.09	7.90 ± 0.11	1.22 ± 0.05	3.24 ± 0.02	3.44 ± 0.06
		2 wk	12	3.37 ± 0.85	3.48 ± 0.10	7.95 ± 0.12	1.25 ± 0.03	3.26 ± 0.03	3.44 ± 0.09
		3 wk	6	3.33 ± 0.96	3.50 ± 0.05	7.97 ± 0.10	1.27 ± 0.03	3.27 ± 0.05	3.43 ± 0.10
		Changes (3 − 0 wk)	NA	−0.35 ± 0.13	0.02 ± 0.06	0.12 ± 0.02	0.08 ± 0.03	0.06 ± 0.04	−0.03 ± 0.07
CON	No lens	0 wk	24	3.47 ± 1.18	3.53 ± 0.28	7.81 ± 0.13	1.21 ± 0.04	3.17 ± 0.03	3.43 ± 0.07
		1 wk	18	3.43 ± 1.13	3.52 ± 0.10	7.94 ± 0.12	1.23 ± 0.04	3.22 ± 0.04	3.49 ± 0.09
		2 wk	12	3.27 ± 1.17	3.53 ± 0.07	7.88 ± 0.15	1.19 ± 0.04	3.24 ± 0.05	3.45 ± 0.08
		3 wk	6	3.25 ± 1.27	3.47 ± 0.07	7.99 ± 0.13	1.25 ± 0.05	3.26 ± 0.04	3.48 ± 0.10
		Changes (3 − 0 wk)	NA	−0.22 ± 0.18	−0.06 ± 0.17	0.17 ± 0.03	0.04 ± 0.02	0.09 ± 0.05	0.05 ± 0.04

* $P < .01$ and † $P < .05$ in CON right eyes compared with LIM right eyes. ACD = anterior chamber depth; AL = axial length; CON = control; CRC = corneal radius of curvature; LIM = lens-induced myopia; LT = lens thickness; NA = not applicable; SER = spherical equivalent refractive error; VCD = vitreous chamber depth.

vitreous chamber depth, and thus axial length than did the control group, which wore plano lenses over the same period.

Refractive Errors

After 1 week, the treated eyes in the experimental group were myopic, but the contralateral eyes of the same group and the eyes of the control group were not. At the end of 3 weeks of induction, the spherical equivalent refractive errors of the negative lens-treated eyes (-1.54 ± 0.60 D) were significantly different ($P = .001$) from those of the contralateral eyes ($+3.33 \pm 0.96$ D) and from the eyes of the control group fitted with plano lenses ($+3.20 \pm 0.97$ D). The mean interocular differences in refraction show a significant myopic shift in the experimental group, which increased over time, that is, -2.03 ± 0.85 , -3.95 ± 0.78 , and -4.87 ± 0.66 D at 1, 2, and 3 weeks, respectively (all, $P < .01$; Fig. 1A).

Vitreous Chamber Depth, Axial Length, and Corneal Radius of Curvature

There were no significant differences in axial length (Table 2) between the right eyes and the left eyes of the control group, even at the end of the 3-week treatment period (8.01 ± 0.24 and 7.99 ± 0.13 mm). Thus, as expected, interocular differences in axial length of the control group showed no significant change over time (0.05 ± 0.04 , 0.03 ± 0.06 , and 0.02 ± 0.13 mm at 1, 2, and 3 weeks, respectively; Fig. 1B). In contrast, the negative

lens-treated eyes showed excessive axial elongations compared with the fellow (contralateral) eyes by the end of the 3-week treatment period (8.47 ± 0.16 vs. 7.97 ± 0.10 mm, $P = .005$). This effect of the -10 D lens on axial elongation is also evident in the interocular axial length differences, which progressively increased over this period in the experimental group (0.19 ± 0.04 , 0.38 ± 0.04 , and 0.50 ± 0.05 mm at 1, 2, and 3 weeks, respectively) and were significantly different from that in the control group (all, $P < .01$).

The -10 D lens-induced axial length elongation was mainly due to the elongation of the vitreous chamber. The interocular vitreous chamber depth differences in the experimental group were significantly larger than the differences in the control group at 1, 2, and 3 weeks (0.37 ± 0.11 , 0.43 ± 0.12 , and 0.50 ± 0.10 vs. 0.03 ± 0.06 , 0.08 ± 0.09 , and 0.06 ± 0.10 mm, respectively). There were no significant intraocular differences in corneal radius of curvature between the experimental and control groups.

Retinal GJD2 Transcript Levels Were Lower in the Experimental Group Than in the Control Group

As expected, before the initiation of the lens treatments, there was no significant difference in *GJD2* transcript levels between the two groups (Fig. 2). However, the relative retinal messenger RNA expression of *GJD2* decreased in negative lens-wearing eyes after initiation of this treatment. Specifically, significantly lower retinal levels of *GJD2* were recorded for the negative lens-treated

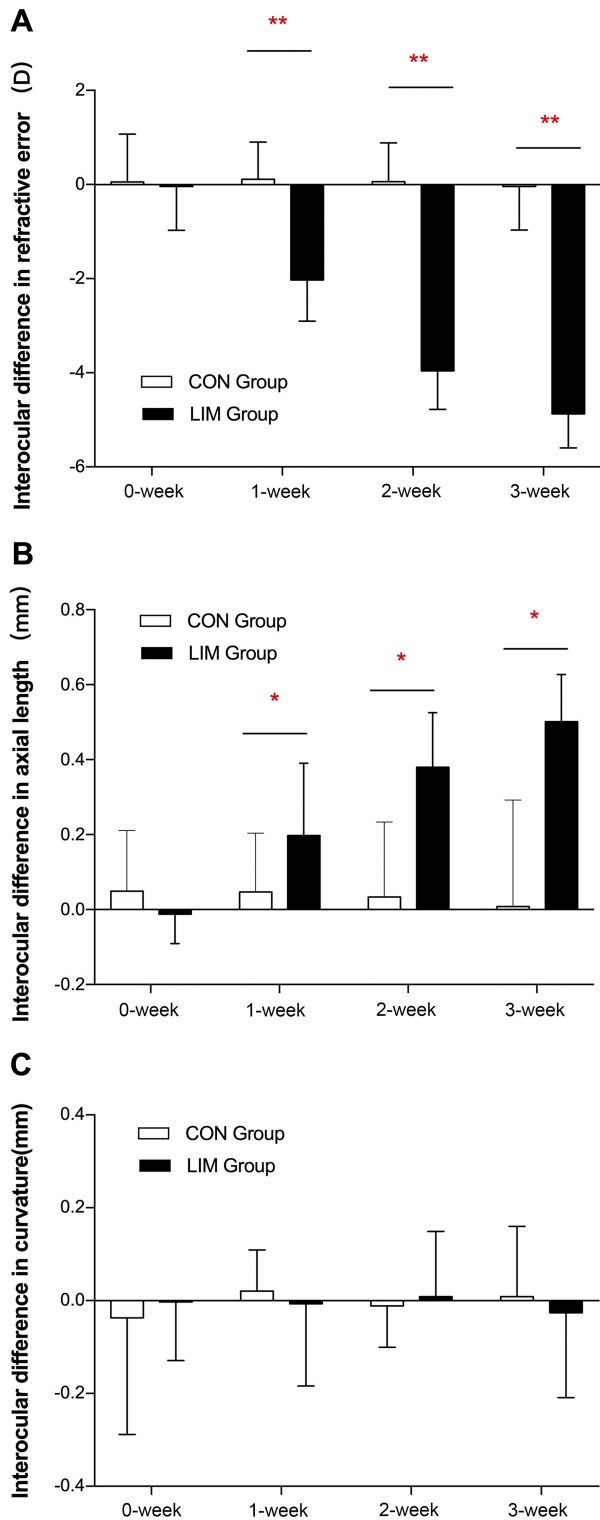


FIGURE 1. Interocular differences (mean ± SEM) in refractive error (in diopters; A), axial length (in millimeters; B), and corneal curvature (in millimeters; C) in guinea pigs fitted with monocular negative lenses (in the experimental group) or plano lenses (in the control group) for 0 to 3 weeks. CON = control; LIM = lens-induced myopia. * $P < .05$ and ** $P < .01$ in the experimental group compared with the control group at each time point. There were 24, 18, 12, and 6 eyes that were measured at 0, 1, 2, and 3 weeks, respectively.

eyes after both 1 and 2 weeks of treatment compared with levels in the retinas of the plano lens-treated eyes ($P = .01$ and $P = .004$, respectively). The corresponding fold changes, that is, normalized to the housekeeping gene, after 0, 1, 2, and 3 weeks of treatment were 1.03, 0.27, 0.18, and 0.76, respectively, in the experimental group and 1.01, 1.01, 1.01, and 1.01, respectively, in the control group.

Retinal Cx36 Protein Expression Levels Were Lower in the Experimental Group Than in the Control Group

Retinal Cx36 protein expression was also decreased in the experimental group compared with the control group, as demonstrated by Western blotting (Fig. 3), although this treatment effect was shorter-lived than the change in *GJD2* gene expression. Thus, although there was no significant difference in retinal Cx36 protein expression between the experimental and control groups at week 0, levels in the experimental group decreased after the initiation of the negative lens treatment, with a significant reduction in expression being observed after 1 week in the experimental group compared with the control group ($P = .01$). Values returned toward the baseline value with longer treatments, and differences between the two groups were also not significant at these later time points. The relative protein levels normalized to β -actin in the experimental group after 0, 1, 2, and 3 weeks of treatment were 1.35, 0.64, 1.14, and 0.90, respectively, whereas the comparable values for the control group were 1.39, 1.36, 1.20, and 1.05, respectively.

Note that the changes in *GJD2* gene messenger RNA and Cx36 protein expression seemed to be asynchronous, with treatment-induced changes in that latter being relatively short-lived compared with

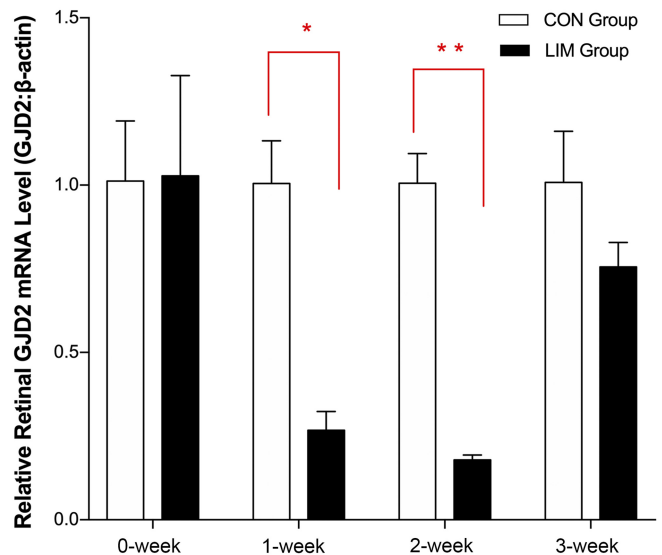


FIGURE 2. Messenger RNA (mRNA) expression of *GJD2* in retina tissues from guinea pigs fitted with monocular negative lenses (in the experimental group) or plano lenses (in the control group) for 0 to 3 weeks. β -Actin served as the housekeeping gene. CON = control; LIM = lens-induced myopia. * $P < .05$ and ** $P < .01$ in the experimental group compared with the control group. Three tissue samples from each group were tested at each time point.

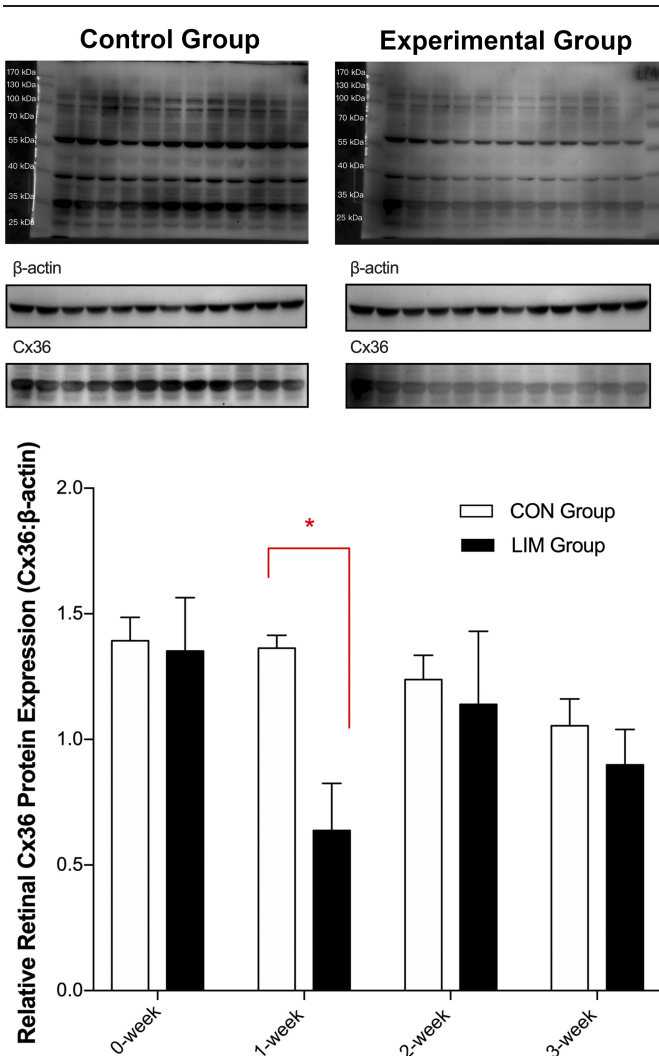


FIGURE 3. Relative Cx36 protein levels in retina tissues from guinea pigs fitted with monocular negative lenses (in the experimental group) or plano lenses (in the control group) for 0 to 3 weeks. β -Actin was used as a reference. CON = control; Cx36 = connexin 36; LIM = lens-induced myopia. * $P < .05$ in the experimental group compared with the control group. Three tissue samples from each group were tested at each time point.

the former gene expression changes. Possible factors contributing to this discrepancy are discussed in the following section.

DISCUSSION

Various studies spanning a range of animal models and experimental techniques have led to a general consensus that emmetropization, the process by which eye growth is adjusted to fine-tune the eye's refractive error, is largely regulated locally, that is, with the eye. For example, in chick studies,³⁹ cutting the optic nerve to eliminate communication between the retina and the brain does not prevent eyes from excessively elongating when exposed to form deprivation or hyperopic defocus stimuli, although subtle differences between the response patterns of animals with intact versus sectioned nerves

have been described in both cases. When form deprivation or defocus stimuli are imposed on only a sector of their retina,^{40–42} these eyes show local shape changes corresponding to the affected retina, offering further evidence for local regulation, initiated in the retina. Thus, exploration of the role of the retinal *GJD2* gene in myopia represents a potentially important step toward elucidating mechanisms underlying the development of myopia.

Similar to findings from other studies that used negative lenses to induced experimental myopia in guinea pigs (Appendix Table A1, available at <http://links.lww.com/OPX/A462>), this study also revealed accelerated eye elongation and myopic shifts in the guinea pigs treated with -10 D lenses.^{39–42} Interestingly, the rate of axial length elongation in lens-induced myopia eyes seemed to slow down slightly over time, with changes in refractive error decreasing in parallel. Thus, compared with mean changes over the first week in the lens-induced myopia group of 0.19 mm and -2.03 D, the equivalent weekly changes in interocular differences in axial length and refractive error for the 2- and 3-week treatment groups are 0.19 and 0.17 mm for axial length and -1.98 and -1.63 D, respectively. It should be noted that the initial age of guinea pigs in the current study was 4 weeks, which is older than that of the animals in previous related studies, whereas the treatment duration was 3 weeks, which is shorter than that of other studies.^{37,43–51} These differences may account, at least in part, for the failure of the guinea pigs in the experimental group to fully compensate to the imposed hyperopic defocus at the end of the study, which was also an intended outcome. There has been one other study reporting on changes in relative *GJD2* messenger RNA expression and Cx36 protein in the retina of guinea pigs, in this case involving form deprivation myopia.⁵² Given the accumulating evidence that the mechanisms underlying form deprivation myopia and lens-induced myopia may be different,¹⁴ our study provided further opportunity to examine the latter question. In relation to differences between form deprivation myopia and lens-induced myopia, these two types of myopia seem to be differentially affected by altered environmental light conditions.^{53–56} For example, although high ambient light levels exert a protective effect against form deprivation myopia in chickens and monkeys,^{53,55} they do not prevent compensation to imposed hyperopic defocus, that is, lens-induced myopia.^{54,56} These two types of myopia seem to be also differentially affected by some pharmacological treatments.⁵⁷ Perhaps of most relevance to the study reported here, there seem to be differences in time-integrated responses to these two types of myopia-inducing stimuli, at least for some experimental animal models.⁵⁸ In relation to the changes in retinal *GJD2* messenger RNA and Cx36 protein expression levels in guinea pigs with form deprivation myopia, both were found to be reduced after the 3-week treatment.⁵² That the changes in relative *GJD2* gene messenger RNA expression in the -10 D lens-treated group were also greatest early in the treatment period, for example, 0.27 and 0.18 for weeks 1 and 2 compared with 0.76 for week 3, may point to differences in the signals responsible for the initiation of myopic growth responses as opposed to the maintenance of these responses. However, it is also possible that the latter reductions may reflect structural changes in the retina, secondary to induced changes in vitreous chamber dimensions, given that eyes experienced hyperopic defocus throughout the 3-week experimental period, albeit reduced in amount by the end of this period.

Apart from targeting lens-induced myopia rather than form deprivation myopia, the current study also documented changes in retinal *GJD2* gene and Cx36 protein expression on a finer timescale.

In contrast to the finding for form deprivation myopia, *GJD2* messenger RNA expression was not significantly altered after 3 weeks of treatment, although significant relative decreases were observed after shorter treatment durations (of 1 and 2 weeks), and Cx36 protein expression was also significantly decreased after 1 week of treatment. Taken together, the results of this and the previous study suggest that the *GJD2* gene is involved in both form deprivation myopia and lens-induced myopia, but the subtle differences in expression patterns open the possibility that some parts of the retinal signal pathway may not be shared.

In studies aimed at elucidating the retinal mechanisms underlying lens-induced myopia, both dopamine regulation and ON-OFF retinal circuits have been investigated.⁵⁷ As Zhou et al.⁵⁷ noted in their review article focusing on the relationship between the dopamine and myopia, most studies have found retinal dopamine levels to be decreased during the development of myopia, even when different myopia animal models were involved. Furthermore, increased retinal dopamine synthesis and release under bright light conditions⁵⁷ offer a plausible explanation for results from other studies showing that high ambient environmental light has protective effects on experimentally induced (animal) myopia.⁵³ One specific study in mice also linked bright light exposure, sufficient to suppress form deprivation myopia, with increased dopamine receptor D₁ activity in the bipolar cells of the ON pathway.⁵⁹ Of relevance to the current study, dopamine regulates the phosphorylation of Cx36. Cx36-containing gap junctions also play an essential role in electrical circuits within the retinal rod system.⁶⁰ During the day when light levels are high, the dopamine D₂ family receptors are activated, and adenylate cyclase activity is inhibited, decreasing Cx36 phosphorylation, which is mediated by cyclic adenosine monophosphate-dependent protein kinase A. The net effect of these changes is a decrease in gap junction conduction, with opposite changes occurring at night.

In the ON pathway in the retina, rod bipolar cells relay signals from rods to All amacrine cells; these signals also travel via Cx36 gap junctions to reach ON cone bipolar cells and finally ON ganglion cells.⁶¹ In the OFF pathway, All amacrine cells are connected with OFF cone bipolar cells via glycinergic inhibitory synapses. Rods are also directly coupled to cones via Cx36 gap junctions.⁶²

Given the wide distribution of Cx36 gap junctions in the retina, the net effect of the observed transient decrease in retinal Cx36 protein expression on retinal signaling warrants further investigation. For example, it is interesting to speculate that Cx36 may be a downstream component of a retinal dopamine signaling pathway regulating myopia. Thus, decreases in retinal dopamine, as linked to experimental myopia, are expected to increase Cx36 phosphorylation. Note also that in both the mouse⁶³ and the rabbit,⁶⁴ the extent of coupling among retina cells via Cx36 gap junctions is directly related to Cx36 phosphorylation rather than changes in the number of gap junctions.

Further studies are warranted to understand the transient reduction in Cx36 protein expression reported here. Such studies could make use of immunochemistry to localize the Cx36 protein in specific retinal layers at timed intervals during lens treatments. Some factors that could have contributed to the small discrepancies in the timing of changes in messenger RNA and protein expression include messenger RNA modifications,⁶⁵ posttranscriptional protein modifications,⁶⁶ and differences in protein turnover or half-life.⁶⁷ The turnover of connexin proteins is known to be influenced by the physiological environment. Is it possible that the turnover rate of Cx36 also varies with the quality of the retinal image and so level of imposed optical defocus, which is expected to vary across the different stages of myopia development.^{68,69} It is also possible that the level of phosphorylated Cx36 may be as or more important, especially in the later stage of myopia development, when the amount of imposed defocus has also been reduced. Could such temporal changes in phosphorylation versus protein expression also explain the different findings of the current lens-induced myopia and previous form-deprivation myopia studies? Advanced *in vivo* electrophysiological recording techniques may be able to offer additional insight into such differences.

In summary, our study found the relative retinal messenger RNA expression of *GJD2* gene decreased over the course of lens-induced myopia, as did Cx36 protein expression. Further investigation of the roles of the *GJD2* gene and Cx36 protein in the signal pathways and mechanisms underlying myopia, a multifactorial disease, is warranted.

ARTICLE INFORMATION

Supplemental Digital Content: Appendix Figure A1 (available at <http://links.lww.com/OPX/A461>). The lenses (−10 D or plano) with four small holes in the peripheral base were sewed to an adhesive tape, attached at their periphery. A lens frame was attached to the other side of the adhesive tape, which was glued to the orbital rim of the eye. The optical center of the lens was aligned with the center of the pupil. Guinea pigs could open their eyes and blink freely while wearing the lenses, without pressure on either their corneas or eyelids.

Appendix Table A1 (available at <http://links.lww.com/OPX/A462>). Ocular biometric parameters, including refractive error and axial length of the negative lens-treated eyes in different studies that used −10 D lens to monocularly induce guinea pig myopia.

Submitted: January 27, 2020

Accepted: July 30, 2020

Funding/Support: The Department of Science and Technology of Sichuan Province (2015SZ0069; to LL).

Conflict of Interest Disclosure: None of the authors have reported a financial conflict of interest.

Study Registration Information: Laboratory Animal Center of Sichuan University (2016038A).

Author Contributions and Acknowledgments: Conceptualization: QZ, FL, LL; Data Curation: QZ, BC, XL; Formal Analysis: QZ, XL; Funding Acquisition: GY, LL; Methodology: QZ, BC, FL, LL; Project Administration: LL; Writing – Original Draft: QZ; Writing – Review & Editing: GY, LL.

The authors thank Dr. Christine F. Wildsoet for her help with the editing of this article.

REFERENCES

1. Foster PJ, Jiang Y. Epidemiology of Myopia. *Eye (Lond)* 2014;28:202–8.
2. Fricke TR, Jong M, Naidoo KS, et al. Global Prevalence of Visual Impairment Associated with Myopic Macular

Degeneration and Temporal Trends from 2000 through 2050: Systematic Review, Meta-analysis and Modelling. *Br J Ophthalmol* 2018;102:855–62.

3. Zheng YF, Pan CW, Chay J, et al. The Economic Cost of Myopia in Adults Aged over 40 Years in Singapore. *Invest Ophthalmol Vis Sci* 2013;54:7532–7.

4. Vitale S, Cotch MF, Sperduto R, et al. Costs of Refractive Correction of Distance Vision Impairment in the United States, 1999–2002. *Ophthalmology* 2006;113:2163–70.

5. Wong TY, Ferreira A, Hughes R, et al. Epidemiology and Disease Burden of Pathologic Myopia and Myopic Choroidal Neovascularization: An Evidence-based Systematic Review. *Am J Ophthalmol* 2014;157:9–25.e12.

6. Flitcroft DI. The Complex Interactions of Retinal, Optical and Environmental Factors in Myopia Aetiology. *Prog Retin Eye Res* 2012;31:622–60.

7. Bourne RR, Stevens GA, White RA, et al. Causes of Vision Loss Worldwide, 1990–2010: A Systematic Analysis. *Lancet Glob Health* 2013;1:e339–49.

8. Smith EL, 3rd, Hung LF, Arumugam B, et al. Effects of Long-wavelength Lighting on Refractive Development in Infant Rhesus Monkeys. *Invest Ophthalmol Vis Sci* 2015;56:6490–500.
9. Metlapally R, Park HN, Chakraborty R, et al. Genome-wide Scleral Micro- and Messenger-RNA Regulation during Myopia Development in the Mouse. *Invest Ophthalmol Vis Sci* 2016;57:6089–97.
10. Wisely CE, Sayed JA, Tamez H, et al. The Chick Eye in Vision Research: An Excellent Model for the Study of Ocular Disease. *Prog Retin Eye Res* 2017; 61:72–97.
11. He L, Frost MR, Siegwart JT, Jr., et al. Altered Gene Expression in Tree Shrew Retina and Retinal Pigment Epithelium Produced by Short Periods of Minus-lens Wear. *Exp Eye Res* 2018;168:77–88.
12. Srinivasalu N, McFadden SA, Medcalf C, et al. Gene Expression and Pathways Underlying Form Deprivation Myopia in the Guinea Pig Sclera. *Invest Ophthalmol Vis Sci* 2018;59:1425–34.
13. Schaeffel F, Feldkaemper M. Animal Models in Myopia Research. *Clin Exp Optom* 2015;98:507–17.
14. Morgan IG, Ashby RS, Nickla DL. Form Deprivation and Lens-induced Myopia: Are They Different? *Ophthalmic Physiol Opt* 2013;33:355–61.
15. Miraldi Utz V. Nature versus Nurture: A Systematic Approach to Elucidate Gene-environment Interactions in the Development of Myopic Refractive Errors. *Ophthalmic Genet* 2017;38:117–21.
16. Solouki AM, Verhoeven VJ, van Duijn CM, et al. A Genome-wide Association Study Identifies a Susceptibility Locus for Refractive Errors and Myopia at 15q14. *Nat Genet* 2010;42:897–901.
17. Chen JH, Chen H, Huang S, et al. Endophenotyping Reveals Differential Phenotype-genotype Correlations between Myopia-associated Polymorphisms and Eye Biometric Parameters. *Mol Vis* 2012;18:765–78.
18. Verhoeven VJ, Hysi PG, Wojciechowski R, et al. Genome-wide Meta-analyses of Multiethnicity Cohorts Identify Multiple New Susceptibility Loci for Refractive Error and Myopia. *Nat Genet* 2013;45:314–8.
19. Cheng CY, Schache M, Ikram MK, et al. Nine Loci for Ocular Axial Length Identified through Genome-wide Association Studies, Including Shared Loci with Refractive Error. *Am J Hum Genet* 2013;93:264–77.
20. Chen CD, Yu ZQ, Chen XL, et al. Evaluating the Association between Pathological Myopia and SNPs in RASGRF1, ACTC1 and GJD2 Genes at Chromosome 15q14 and 15q25 in a Chinese Population. *Ophthalmic Genet* 2015;36:1–7.
21. Hervé JC, Derangeon M. Gap-junction-mediated Cell-to-cell Communication. *Cell Tissue Res* 2013; 352:21–31.
22. Volgyi B, Kovacs-Oller T, Atlasz T, et al. Gap Junctional Coupling in the Vertebrate Retina: Variations on One Theme? *Prog Retin Eye Res* 2013;34:1–18.
23. Kovács-Öller T, Debortin G, Balogh M, et al. Connexin36 Expression in the Mammalian Retina: A Multiple-species Comparison. *Front Cell Neurosci* 2017; 11:65.
24. Feigenspan A, Janssen-Bienhold U, Hormuzdi S, et al. Expression of Connexin36 in Cone Pedicles and OFF-cone Bipolar Cells of the Mouse Retina. *J Neurosci* 2004;24:3325–34.
25. Hansen KA, Torborg CL, Elstrott J, et al. Expression and Function of the Neuronal Gap Junction Protein Connexin 36 in Developing Mammalian Retina. *J Comp Neurol* 2005;493:309–20.
26. Hidaka S, Akahori Y, Kurosawa Y. Dendrodendritic Electrical Synapses between Mammalian Retinal Ganglion Cells. *J Neurosci* 2004;24:10553–67.
27. Roy K, Kumar S, Bloomfield SA. Gap Junctional Coupling between Retinal Amacrine and Ganglion Cells Underlies Coherent Activity Integral to Global Object Perception. *Proc Natl Acad Sci U S A* 2017;114: E10484–93.
28. Ivanova E, Yee CW, Baldoni R, Jr., et al. Aberrant Activity in Retinal Degeneration Impairs Central Visual Processing and Relies on Cx36-containing Gap Junctions. *Exp Eye Res* 2016;150:81–9.
29. Gawne TJ, Siegwart JT, Jr., Ward AH, et al. The Wavelength Composition and Temporal Modulation of Ambient Lighting Strongly Affect Refractive Development in Young Tree Shrews. *Exp Eye Res* 2017;155: 75–84.
30. Wang M, Schaeffel F, Jiang B, et al. Effects of Light of Different Spectral Composition on Refractive Development and Retinal Dopamine in Chicks. *Invest Ophthalmol Vis Sci* 2018;59:4413–24.
31. Kihara AH, de Castro LM, Moriscot AS, et al. Prolonged Dark Adaptation Changes Connexin Expression in the Mouse Retina. *J Neurosci Res* 2006;83: 1331–41.
32. Teves M, Shi Q, Stell WK, et al. The Role of Cell-cell Coupling in Myopia Development and Light Adaptation. *Invest Ophthalmol Vis Sci* 2014;55:3036.
33. Li W, Lan W, Yang S, et al. The Effect of Spectral Property and Intensity of Light on Natural Refractive Development and Compensation to Negative Lenses in Guinea Pigs. *Invest Ophthalmol Vis Sci* 2014;55: 6324–32.
34. Li H, Wu J, Cui D, et al. Retinal and Choroidal Expression of BMP-2 in Lens-induced Myopia and Recovery from Myopia in Guinea Pigs. *Mol Med Rep* 2016; 13:2671–6.
35. Zi Y, Deng Y, Zhao J, et al. Morphologic and Biochemical Changes in the Retina and Sclera Induced by Form Deprivation High Myopia in Guinea Pigs. *BMC Ophthalmol* 2020;20:105.
36. Liu Y, Wang Y, Lv H, et al. α -adrenergic Agonist Brimonidine Control of Experimentally Induced Myopia in Guinea Pigs: A Pilot Study. *Mol Vis* 2017;23: 785–98.
37. Geng C, Li Y, Guo F, et al. RNA Sequencing Analysis of Long Non-coding RNA Expression in Ocular Posterior Poles of Guinea Pig Myopia Models. *Mol Vis* 2020;26: 117–34.
38. Zhou X, Qu J, Xie R, et al. Normal Development of Refractive State and Ocular Dimensions in Guinea Pigs. *Vision Res* 2006;46:2815–23.
39. Wildsoet C, Pettigrew JJ. Experimental Myopia and Anomalous Eye Growth Patterns Unaffected by Optic Nerve Section in Chickens: Evidence for Local Control of Eye Growth. *Clin Vis Sci* 1988;3:99–107.
40. Smith EL, 3rd, Huang J, Hung LF, et al. Hemiretinal Form Deprivation: Evidence for Local Control of Eye Growth and Refractive Development in Infant Monkeys. *Invest Ophthalmol Vis Sci* 2009;50:5057–69.
41. Zeng G, McFadden SA. Regional Variation in Susceptibility to Myopia from Partial Form Deprivation in the Guinea Pig. *Invest Ophthalmol Vis Sci* 2010; 51:1736.
42. Chu CH, Deng L, Kee CS. Effects of Hemiretinal Form Deprivation on Central Refractive Development and Posterior Eye Shape in Chicks. *Vision Res* 2012; 55:24–31.
43. Dong L, Shi XH, Kang YK, et al. Ocular Size and Shape in Lens-induced Myopia in Young Guinea Pigs. *BMC Ophthalmol* 2019;19:102.
44. Zhao W, Bi AL, Xu CL, et al. GABA and GABA Receptors Alterations in the Primary Visual Cortex of Concave Lens-induced Myopic Model. *Brain Res Bull* 2017; 130:173–9.
45. Guoping L, Xiang Y, Jianfeng W, et al. Alterations of Glutamate and γ -aminobutyric Acid Expressions in Normal and Myopic Eye Development in Guinea Pigs. *Invest Ophthalmol Vis Sci* 2017;58:1256–65.
46. Qian L, Zhao H, Li X, et al. Pirenzepine Inhibits Myopia in Guinea Pig Model by Regulating the Balance of MMP-2 and TIMP-2 Expression and Increased Tyrosine Hydroxylase Levels. *Cell Biochem Biophys* 2015;71: 1373–8.
47. Sha F, Ye X, Zhao W, et al. Effects of Electroacupuncture on the Levels of Retinal Gamma-aminobutyric Acid and Its Receptors in a Guinea Pig Model of Lens-induced Myopia. *Neuroscience* 2015;287:164–74.
48. Chen BY, Wang CY, Chen WY, et al. Altered TGF- β 2 and bFGF Expression in Scleral Desmocytes from an Experimentally-induced Myopia Guinea Pig Model. *Graefes Arch Clin Exp Ophthalmol* 2013;251:1133–44.
49. Chen BY, Ma JX, Wang CY, et al. Mechanical Behavior of Scleral Fibroblasts in Experimental Myopia. *Graefes Arch Clin Exp Ophthalmol* 2012;250:341–8.
50. Jiang WJ, Song HX, Li SY, et al. Amphiregulin Antibody and Reduction of Axial Elongation in Experimental Myopia. *EBioMedicine* 2017;17:134–44.
51. Guo D, Ding M, Song X, et al. Regulatory Roles of Differentially Expressed MicromRNAs in Metabolic Processes in Negative Lens-induced Myopia Guinea Pigs. *BMC Genomics* 2020;21:13.
52. Yang GY, Liu FY, Li X, et al. Decreased Expression of Gap Junction Delta-2 (GJD2) Messenger RNA and Connexin 36 Protein in Form-deprivation Myopia of Guinea Pigs. *Chin Med J (Engl)* 2019;132:1700–5.
53. Smith EL, 3rd, Hung LF, Huang J. Protective Effects of High Ambient Lighting on the Development of Form-deprivation Myopia in Rhesus Monkeys. *Invest Ophthalmol Vis Sci* 2012;53:421–8.
54. Smith EL, 3rd, Hung LF, Arumugam B, et al. Negative Lens-induced Myopia in Infant Monkeys: Effects of High Ambient Lighting. *Invest Ophthalmol Vis Sci* 2013; 54:2959–69.
55. Ashby R, Ohlendorf A, Schaeffel F. The Effect of Ambient Illuminance on the Development of Deprivation Myopia in Chicks. *Invest Ophthalmol Vis Sci* 2009;50: 5348–54.
56. Ashby RS, Schaeffel F. The Effect of Bright Light on Lens Compensation in Chicks. *Invest Ophthalmol Vis Sci* 2010;51:5247–53.
57. Zhou X, Pardue MT, Iuvone PM, et al. Dopamine Signaling and Myopia Development: What Are the Key Challenges. *Prog Retin Eye Res* 2017;61:60–71.
58. Kee CS, Marzani D, Wallman J. Differences in Time Course and Visual Requirements of Ocular Responses to Lenses and Diffusers. *Invest Ophthalmol Vis Sci* 2001; 42:575–83.
59. Chen S, Zhi Z, Ruan Q, et al. Bright Light Suppresses Form-deprivation Myopia Development with Activation of Dopamine D₁ Receptor Signaling in the ON Pathway in Retina. *Invest Ophthalmol Vis Sci* 2017; 58:2306–16.
60. Guldenagel M, Ammermuller J, Feigenspan A, et al. Visual Transmission Deficits in Mice with Targeted

Disruption of the Gap Junction Gene Connexin36. *J Neurosci* 2001;21:6036–44.

61. Feigenspan A, Teubner B, Willecke K, et al. Expression of Neuronal Connexin36 in All Amacrine Cells of the Mammalian Retina. *J Neurosci* 2001; 21:230–9.

62. Sohl G, Jousseaume A, Kociok N, et al. Expression of Connexin Genes in the Human Retina. *BMC Ophthalmol* 2010;10:27.

63. Li H, Zhang Z, Blackburn MR, et al. Adenosine and Dopamine Receptors Coregulate Photoreceptor Coupling

via Gap Junction Phosphorylation in Mouse Retina. *J Neurosci* 2013;33:3135–50.

64. Kothmann WW, Massey SC, O'Brien J. Dopamine-stimulated Dephosphorylation of Connexin 36 Mediates All Amacrine Cell Uncoupling. *J Neurosci* 2009; 29:14903–11.

65. Roundtree IA, Evans ME, Pan T, et al. Dynamic RNA Modifications in Gene Expression Regulation. *Cell* 2017;169:1187–200.

66. Kuhar MJ. On the Use of Protein Turnover and Half-lives. *Neuropsychopharmacology* 2009;34:1172–3.

67. Inose H, Ochi H, Kimura A, et al. A MicroRNA Regulatory Mechanism of Osteoblast Differentiation. *Proc Natl Acad Sci U S A* 2009;106:20794–9.

68. Fernandes R, Girao H, Pereira P. High Glucose Down-regulates Intercellular Communication in Retinal Endothelial Cells by Enhancing Degradation of Connexin 43 by a Proteasome-dependent Mechanism. *J Biol Chem* 2004;279:27219–24.

69. Wang HY, Lin YP, Mitchell CK, et al. Two-color Fluorescent Analysis of Connexin 36 Turnover: Relationship to Functional Plasticity. *J Cell Sci* 2015;128:3888–97.